J|A|C|S ARTICLES

Published on Web 08/30/2010

Acceptor Energy Level Control of Charge Photogeneration in Organic Donor/Acceptor Blends

Safa Shoaee,[†] Tracey M. Clarke,[†] Chun Huang,[‡] Stephen Barlow,[‡] Seth R. Marder,[‡] Martin Heeney,[§] Iain McCulloch,[†,§] and James R. Durrant*[,†]

Centre for Plastic Electronics, Department of Chemistry, Imperial College London, London, SW7 2AZ United Kingdom, School of Chemistry & Biochemistry and Center for Organic Photonics and Electronics, Georgia Institute of Technology, 901 Atlantic Drive, Atlanta, Georgia 30332-0400, and Merck Chemicals, Chilworth Science Park, Southampton SO16 7QD, United Kingdom

Received May 18, 2010; E-mail: j.durrant@imperial.ac.uk; seth.marder@chemistry.gatech.edu

Abstract: In this paper we focus upon the role of interfacial energetics in influencing the separation of charge transfer states into dissociated charge carriers in organic donor/acceptor blend films. In particular, we undertake transient optical studies of films comprising regioregular poly(3-hexylthiophene) (P3HT) blended with a series of perylene-3,4:9,10-tetracarboxydiimide (PDI) electron acceptors. For this film series, we observe a close correlation between the PDI electron affinity and the efficiency of charge separation. This correlation is discussed in the context of studies of charge photogeneration for other organic donor/acceptor blend films, including other polymers, blend compositions, and the widely used electron acceptor 3′-phenyl-3′*H*-cyclopropa[1,9](C_{60}-I_h)[5,6]fullerene-3′-butanoic acid methyl ester (PCBM).

Introduction

Organic donor/acceptor blend films are attracting increasing interest for photovoltaic solar energy conversion, with reported device efficiencies now exceeding 6%.[1−3] The function of such devices is based on photoinduced charge separation at the donor/acceptor interface as illustrated in Figure 1. The efficiency of charge photogeneration in organic donor/acceptor blend films has been reported to depend on a range of factors, including film nanomorphology,[4−11] the presence of macroscopic electric fields,[12−14] the dielectric constant of the blend,[4,15,16] charge-carrier mobilities,[4,7,17−21] the free-energy difference driving charge separation (ΔG_{CS}),[21−23] and the strength of electronic interactions at the donor/acceptor interface.[24] There is increasing evidence that the efficiency of this charge-separation process can be determined by the presence of Coulombically bound charge-

[†] Imperial College London.
[‡] Georgia Institute of Technology.
[§] Merck Chemicals.

(1) Kim, J. Y.; Lee, K.; Coates, N. E.; Moses, D.; Nguyen, T.-Q.; Dante, M.; Heeger, A. J. *Science* **2007**, *317*, 222.
(2) Park, S. H.; Roy, A.; Beaupre, S.; Cho, S.; Coates, N.; Moon, J. S.; Moses, D.; Leclerc, M.; Lee, K.; Heeger, A. J. *Nat. Photonics* **2009**, *3*, 297.
(3) Peet, J.; Kim, J. Y.; Coates, N. E.; Ma, W. L.; Moses, D.; Heeger, A. J.; Bazan, G. C. *Nat. Mater.* **2007**, *6*, 497.
(4) Mihailetchi, V. D.; Koster, L. J. A.; Blom, P. W. M.; Melzer, C.; de Boer, B.; van Duren, J. K. J.; Janssen, R. A. J. *Adv. Funct. Mater.* **2005**, *15*, 795.
(5) Chasteen, S. V.; Sholin, V.; Carter, S. A.; Rumbles, G. *Sol. Energy Mater. Sol. Cells* **2008**, *92*, 651.
(6) Hoppe, H.; Glatzel, T.; Niggemann, M.; Schwinger, W.; Schaeffler, F.; Hinsch, A.; Lux-Steiner, M. C.; Sariciftci, N. S. *Thin Solid Films* **2006**, *511−512*, 587.
(7) Quist, P. A. C.; Martens, T.; Manca, J. V.; Savenije, T. J.; Siebbeles, L. D. A. *Sol. Energy Mater. Sol. Cells* **2006**, *90*, 362.
(8) Zhang, F.; Jespersen, K. G.; Björström, C.; Svensson, M.; Andersson, M. R.; Sundström, V.; Magnusson, K.; Moons, E.; Yartsev, A.; Inganäs, O. *Adv. Funct. Mater.* **2006**, *16*, 667.
(9) Müller, J. G.; Lupton, J. M.; Feldmann, J.; Lemmer, U.; Scharber, M. C.; Sariciftci, N. S.; Brabec, C. J.; Scherf, U. *Phys. Rev. B* **2005**, *72*, 195208.
(10) Shaheen, S. E.; Brabec, C. J.; Sariciftci, N. S.; Padinger, F.; Fromherz, T.; Hummelen, J. C. *Appl. Phys. Lett.* **2001**, *78*, 841.
(11) Blom, P. W. M.; Mihailetchi, V. D.; Koster, L. J. A.; Markov, D. E. *Adv. Mater.* **2007**, *19*, 1551.
(12) Offermans, T.; van Hal, P. A.; Meskers, S. C. J.; Koetse, M. M.; Janssen, R. A. J. *Phys. Rev. B* **2005**, *72*, 045213.
(13) Veldman, D.; Opek, O.; Meskers, S. C. J.; Sweelssen, J.; Koetse, M. M.; Veenstra, S. C.; Kroon, J. M.; Bavel, S. S. v.; Loos, J.; Janssen, R. A. J. *J. Am. Chem. Soc.* **2008**, *130*, 7721.
(14) Mihailetchi, V. D.; Koster, L. J. A.; Hummelen, J. C.; Blom, P. W. M. *Phys. Rev. Lett.* **2004**, *93*, 216601.
(15) Mandoc, M. M.; Veurman, W.; Sweelssen, J.; Koetse, M. M. *Appl. Phys. Lett.* **2007**, *91*, 073518.
(16) Lenes, M.; Kooistra, F. B.; Hummelen, J. C.; Severen, I. V.; Lutsen, L.; Vanderzande, D.; Cleij, T. J.; Blom, P. W. M. *J. Appl. Phys.* **2008**, *104*, 114517.
(17) Hoppe, H.; Sariciftci, N. S. *J. Mater. Chem.* **2006**, *16*, 45.
(18) Reyes-Reyes, M.; Kim, K.; Carroll, D. L. *Appl. Phys. Lett.* **2005**, *87*, 083506.
(19) Li, G.; Shrotriya, V.; Yao, Y.; Yang, Y. *J. Appl. Phys.* **2005**, *98*, 043704.
(20) McNeill, C. R.; Halls, J. J. M.; Wilson, R.; Whiting, G. L.; Berkebile, S.; Ramsey, M. G.; Friend, R. H.; Greenham, N. C. *Adv. Funct. Mater.* **2008**, *18*, 2309.
(21) (a) Shoaee, S.; An, Z.; Zhang, X.; Barlow, S.; Marder, S. R.; Duffy, W.; Heeney, M.; McCulloch, I.; Durrant, J. R. *Chem. Commun.* **2009**, 5445. (b) Howard, I. L., F.; Keivanidis, P.; Friend, R.; Greenham, N. *J. Phys. Chem. C* **2009**, *113*, 21225.
(22) Ohkita, H.; Cook, S.; Astuti, Y.; Duffy, W.; Tierney, S.; Zhang, W.; Heeney, M.; McCulloch, I.; Nelson, J.; Bradley, D. D. C.; Durrant, J. R. *J. Am. Chem. Soc.* **2008**, *130*, 3030.
(23) Clarke, T. M.; Ballantyne, A. M.; Nelson, J.; Bradley, D. D. C.; Durrant, J. R. *Adv. Funct. Mater.* **2008**, *18*, 4029.
(24) Nelson, J.; Kirkpatrick, J.; Ravirajan, P. *Phys. Rev. B* **2004**, *69*, 035337.

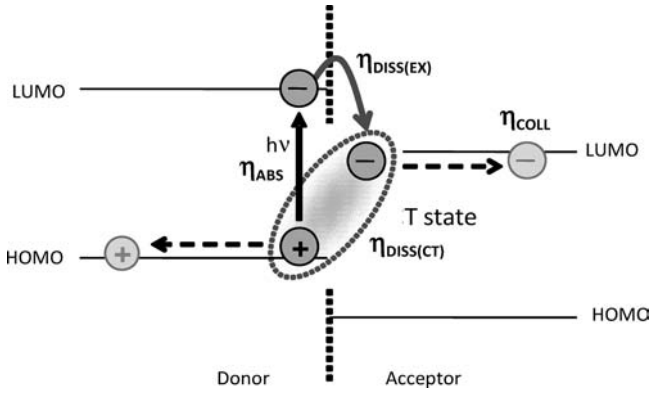

Figure 1. Energy level diagram of a donor/acceptor interface showing a simplified viewpoint of photoexcitation of an electron into the donor LUMO (with efficiency η_{ABS}), followed by exciton dissociation via electron transfer into the acceptor LUMO ($\eta_{DISS(EX)}$) and migration of the separated charges away from the interface (η_{COLL}). Also illustrated is the potential for the electron transfer initially to generate a Coulombically bound charge transfer (CT) state that also requires dissociation ($\eta_{DISS(CT)}$) before the free charge carriers can be collected.

transfer (CT) states at the donor/acceptor interface.[4,12,13,22,23,25−30,54] Such studies have typically concluded that the efficiency of dissociation of the CT state into free charge carriers, illustrated as $\eta_{DISS(CT)}$ in Figure 1, is a crucial factor determining the charge photogeneration yield and thus device photocurrent densities. We note that such CT states are variously referred to in the literature as bound radical or polaron pairs, "exciplexes" (when radiatively coupled to the ground state) or "geminate ion pairs". However, at present there is little consensus concerning the relative importance of the different factors potentially influencing charge photogeneration, and in particular how the efficiency of charge photogeneration can be related to, or predicted from, specific materials properties.

The observation of clear materials structure/charge photogeneration relationships depends critically upon the selection of a suitable materials series. In particular, the observation of a correlation between charge photogeneration and a specific materials property is only possible if other materials properties potentially influencing charge photogeneration are relatively invariant for the series studied. We have previously conducted studies of the yield of the charge-photogeneration process for a series of polythiophenes blended with PCBM.[22] In this materials series, we observed a correlation between the energy levels of the polythiophene donors and the yield of dissociated charge carriers, as quantified by the magnitude of photoinduced absorption of these charges (ΔOD measured at a time delay of 1 μs) determined by high sensitivity transient absorption spectroscopy. More specifically, we observed a correlation between ΔOD and the energetic driving force for charge separation, ΔG_{CS}^{eff}, defined as $\Delta G_{CS}^{eff} = E_S - (IP_D - EA_A)$ where E_S is the energy of the polymer singlet exciton, IP_D the ionization potential of the donor and EA_A the electron affinity of the acceptor. It was proposed that this correlation was consistent with a model in which efficient charge separation was dependent upon the initially generated charge-transfer state possessing sufficient excess thermal energy provided by ΔG_{CS}^{eff}, to overcome the Coulombic binding of this CT state, resulting in a high value for $\eta_{DISS(CT)}$. This model is analogous to Onsager's Theory of charge separation, which is based upon the concept that the efficiency of separation of photogenerated geminate charge pairs is dependent upon the relative magnitudes of their thermalisation length versus their coulomb capture radius. It has been previously suggested that a large LUMO−LUMO offset ($\sim\Delta G_{CS}^{eff}$) at organic donor/acceptor interface will produce a greater thermalisation length,[31] which, in turn, would increase the probability of separation of the bound radical pairs into the fully dissociated charge carriers. The dependence of charge separation upon ΔG_{CS}^{eff} observed by Okhita et al.[22] has important implications for materials design as it suggested, at least for the polythiophene/PCBM series studied, that a relatively large free-energy loss (0.9 eV) was required to drive efficient charge separation.

We have subsequently extended our studies of charge photogeneration to other donor polymers,[25,28,32,33] blend compositions[26,28] and the effect of thermal annealing.[23] In these studies, further correlations between ΔG_{CS} and charge photogeneration were observed, as well as additional effects attributed to the influence of film nanomorphology and the charge-transfer character of the polymer exciton. In this paper we focus upon the role of acceptor electron affinity in determining the efficiency of charge photogeneration and specifically $\eta_{DISS(CT)}$. In particular we study charge photogeneration in films comprising 1:1 blends of P3HT with a series of different perylene diimide derivatives (PDI_x, Chart 1) with varying electron affinities in order to investigate the role of the electron acceptor on ΔG_{CS} and thus charge separation.

Perylenes are attractive model electron acceptors for studies of charge photogeneration in donor/acceptor blends as their energetics can be readily modified by chemical substituents and they exhibit a well-defined and high-oscillator-strength anion absorption band (extinction coefficient $\varepsilon \approx 80\,000$ M^{-1} cm^{-1} compared to that of P3HT $\sim 20\,000$ M^{-1} cm^{-1}). They have, moreover, already received significant attention for applications in dye-sensitized and vacuum-deposited solar cells,[34−38] although their performance in organic polymer/perylene blend devices has been relatively poor to date, a result that has typically been attributed to unfavorable nanomorphologies for charge transport to the device electrodes. We have previously reported a comparison of charge photogeneration between polythiophene:PCBM blend films and the same polythiophenes blended with one perylene diimide electron acceptor (PDI_2 in Chart 1). It was observed that for equivalent values of ΔG_{CS}^{eff}, the PDI_2 acceptor achieved higher charge generation efficiency

(25) Clarke, T.; Ballantyne, A.; Jamieson, F.; Brabec, C.; Nelson, J.; Durrant, J. *Chem. Commun.* **2009**, 89.
(26) Keivanidis, P.; Clarke, T.; Lilliu, S.; Agostinelli, T.; Macdonald, J.; Durrant, J.; Bradley, D.; Nelson, J. *J Phys Chem Lett* **2010**, *1*, 734.
(27) Tvingstedt, K.; Vandewal, K.; Gadisa, A.; Zhang, F.; Manca, J.; Inganaîs, O. *J. Am. Chem. Soc.* **2009**, *131*, 11819.
(28) Clarke, T. M.; Ballantyne, A. M.; Tierney, S.; Heeney, M.; Duffy, W.; McCulloch, I.; Nelson, J.; Durrant, J. R. *J. Phys. Chem. C* **2010**.
(29) Yin, C.; Kietzke, T.; Neher, D.; Horhold, H.-H. *Appl. Phys. Let.* **2007**, *90*, 092117.
(30) Hertel, D.; Soh, E. V.; Bässler, H.; Rothberg, L. J. *Chem. Phys. Let.* **2002**, *361*, 99.
(31) Peumans, P.; Forrest, S. R. *Chem. Phys. Lett.* **2004**, *398*, 27.
(32) Clarke, T. M.; Jamieson, F. C.; Durrant, J. R. *J. Phys. Chem. C* **2009**, *113*, 20934.
(33) Benson-Smith, J. J.; Goris, L.; Vandewal, K.; Haenen, K.; Manca, J. V.; Vanderzande, D.; Bradley, D. D. C.; Nelson, J. *Adv. Funct. Mater.* **2007**, *17*, 451.
(34) Tang, C. W. *Appl. Phys. Lett.* **1986**, *48*, 183.
(35) Ferrere, S.; Gregg, B. A. *New J. Chem.* **2002**, *26*, 1155.
(36) Takahashi, K.; Nakajima, I.; Imoto, K.; Yamaguchi, T.; Komura, T.; Murata, K. *Sol. Energy Mater. Sol. Cells* **2003**, *76*, 115.
(37) Signerski, R. *J. Non-Cryst. Solids* **2006**, *352*, 4319.
(38) Nakamura, J.; Yokoe, C; Mruata, K; Takahashi, K. *J. Appl. Phys.* **2004**, *96*, 6878.

Chart 1. Molecular Structure of PDI_X Derivatives[a]

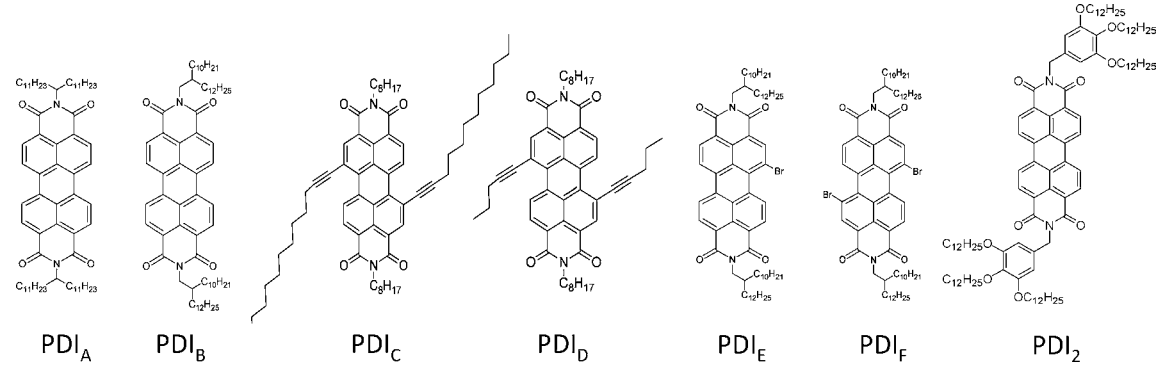

[a] X = A−F starting from left, and PDI_2 at the far right.

Table 1. Properties of the P3HT:PDI_X Blends

blend (P3HT:PDI_X)	EA (eV)[a]	ΔG_{CS}^{eff} (eV)[b]	ΔOD[c]	PLQ (%)[d]	ΔOD/PLQ
PDI_A	3.52	0.72	4.2×10^{-4}	0.86	4.8×10^{-4}
PDI_B	3.55	0.72	5.1×10^{-4}	0.92	4.7×10^{-4}
PDI_C	3.55	0.75	3.7×10^{-4}	0.70	5.3×10^{-4}
PDI_D	3.56	0.76	5.0×10^{-4}	0.90	5.6×10^{-4}
PDI_E	3.59	0.79	5.1×10^{-4}	0.83	6.2×10^{-4}
PDI_F	3.64	0.84	3.1×10^{-4}	0.88	4.5×10^{-4}
PDI2	3.50	0.70	2.9×10^{-4}	0.70	4.1×10^{-4}

[a] Estimated electron affinities evaluated by cyclic voltammetry from the peak value. [b] ΔG_{CS} estimated as E_S − (IP − EA), where IP is the ionization potential of the polymer evaluated by an ambient ultraviolet photoelectron spectroscopy technique (4.8 eV for P3HT) and E_S the singlet exciton energy of the donor, measured from the intercept of the normalized absorption and emission spectra. [c] ΔOD evaluated from the amplitude of the transient absorbance power-law decay phase at 1 μs (λ_{probe} = 700 nm), after correction for the ground state absorbance at the excitation wavelength. [d] Steady-state PL quenching of the blend film relative to the corresponding pristine polymer film.

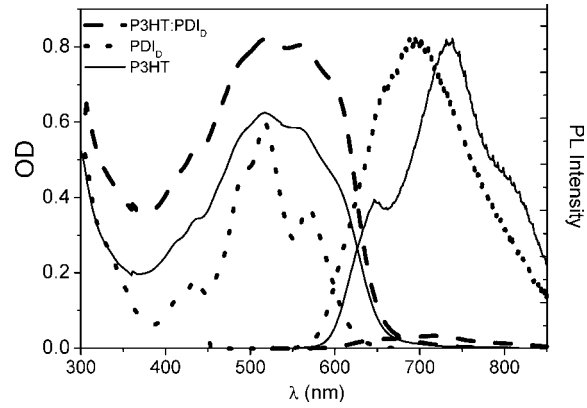

Figure 2. Absorption and photoluminescence spectra measured for the following neat and blend films: PDI_D, P3HT, and (1:1) P3HT:PDI_D. The PL spectra were measured using 500 nm excitation.

than PCBM. This was tentatively assigned as a result of the higher electron mobility of this PDI relative to PCBM,[21] and indicates that, if charge collection limitations can be addressed, such PDIs may be an attractive alternative to PCBM in organic blend solar cells. In the study reported herein, we extend these results to a series of PDIs with electron affinities ranging between 3.50 and 3.64 eV. A remarkably close correlation between ΔG_{CS}^{eff} and charge photogeneration efficiency is demonstrated for this materials series.

Results

The relative electron affinities of the PDI_X series of electron acceptors were estimated by cyclic voltammetry (see the Supporting Information for experimental details). In all cases, reversible reduction waves were observed. The resultant estimated electron affinities of the acceptors are detailed in Table 1 and indicate that electron affinity varies by 140 meV between these electron acceptors. It should be noted that this estimate of EA assumes that the solid-state polarization energies and solvation effects are constant for all the PDIs. The PDIs were all found to blend readily with P3HT, resulting in high optical quality films. Measurements were performed on nonannealed (unless stated otherwise) spin coated films of P3HT:PDI_X blends in a 1:1 ratio by weight prepared from chloroform solutions (see experimental for full details).

Typical absorption spectra of the neat materials and blend films are presented in Figure 2. It is apparent that the PDI absorption spectra overlap significantly with that of P3HT, implying that photoexcitation of the blends will produce both P3HT and PDI excitons. Photoluminescence (PL) data were collected to evaluate the efficiency of exciton quenching for all blend films. Typical PL data observed for the P3HT:PDI_X blends, represented by that for PDI_D, are shown in Figure 2, as well as those for the corresponding pristine films. Consideration of such absorption and emission spectra indicate that for all P3HT:PDI_X blends, the lowest singlet exciton is that of P3HT. Consistent with this observation, the PDI emission was very strongly quenched (>99%) for all blend films (with the exception of PDI_2, see below) relative to that of neat PDI films, suggesting rapid energy transfer from PDI to P3HT. As such, charge photogeneration most likely occurs via electron transfer from the P3HT singlet excitons, as we discuss further below. Weak residual P3HT PL was observed in the blend films, corresponding to 70−92% PL quenching compared to the corresponding neat P3HT films (determined by integration over the emission band), as detailed in Table 1.

We turn to morphology studies of these blend films. Both atomic force microscopy (AFM; Figure S1) and transmission electron microscopy (TEM; Figure 3) data indicate that P3HT:PDI_D blends show small PDI features on the order of tens of nanometers, which are well dispersed within the P3HT phase. With the exception of films employing PDI_2, similar data were obtained for other P3HT:PDI_X films, consistent with our observation of efficient PDI PL quenching and reasonably efficient P3HT PL quenching. The TEM data for the P3HT:PDI_D films show clear evidence for the crystallinity of the small PDI domains, consistent with the absorption spectra and the

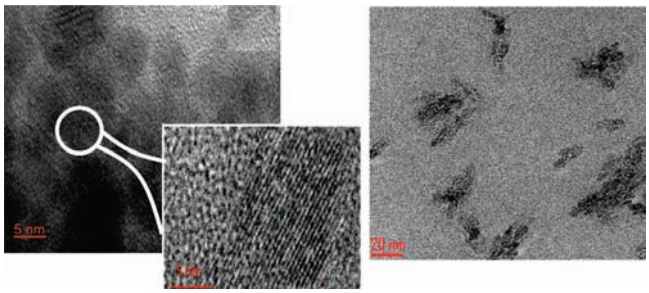

Figure 3. TEM micrographs of P3HT:PDI_D (left) film (expanded region, center: crystallization of PDI_D lattice) and P3HT:PDI_2 (right).

well-established tendency of PDIs to undergo π stacking. The lattice spacing of the PDI_D crystallites was determined from these TEM images to be 0.6 nm, typical of that observed for PDI crystallites.[39] The morphology of the P3HT:PDI_D blend is consistent with that observed by Friend's group[40] where polymer:PDI blends studied show small features of the order of tens of nanometers and some evidence of perylene aggregation in the case of a P3HT:PDI blend.

In contrast to the other perylenes, morphology studies of P3HT:PDI_2 blend films show the formation of large PDI_2 aggregates, with phase segregation on the scale of a few hundreds of nanometers and roughness leading to some features that rise 500−600 nm out of the plane of the film (see Figure 3 and S1). The greater phase segregation observed for P3HT:PDI_2 compared to PDI_D belnd is consistent with the observed less efficient PDI PL quenching we observe in these blend films (70% relative to pristine PDI_2 films). As the processing conditions for all films were constant, the formation of these larger domains may be attributed to the presence of the trialkoxy phenyl groups.

As we have shown previously,[22] exciton PL quenching is only an indicator of the efficiency of exciton quenching at the donor/acceptor interface and is not a reliable measure of the yield of fully dissociated charges. In particular, it is insensitive to the potential for geminate recombination of initially generated polaron pairs (or "charge-transfer" states) prior to their dissociation into separated charges. As such PL quenching can only provide an indication of an upper limit to the charge photogeneration yield. We have previously demonstrated that high sensitivity, micro- to millisecond transient absorption spectroscopy (TAS) can beemployed to monitor the yield of dissociated polarons in such donor/acceptor blend films.[21,22] Full experimental details are given in the Supporting Information, with all experiments reported herein employing an excitation wavelength of 520 nm. Consistent with previous reports,[41] the transient spectrum of all P3HT:PDI_X films exhibited a well-defined absorption maximum at approximately 700 nm indicative of the formation of PDI anions[42,43] as well as a weaker, broad absorption between 900 and 1000 nm assigned to P3HT cations[23,44−47](shown for the P3HT:PDI_D blend film in the inset of Figure 4). Typical decay dynamics of these transient

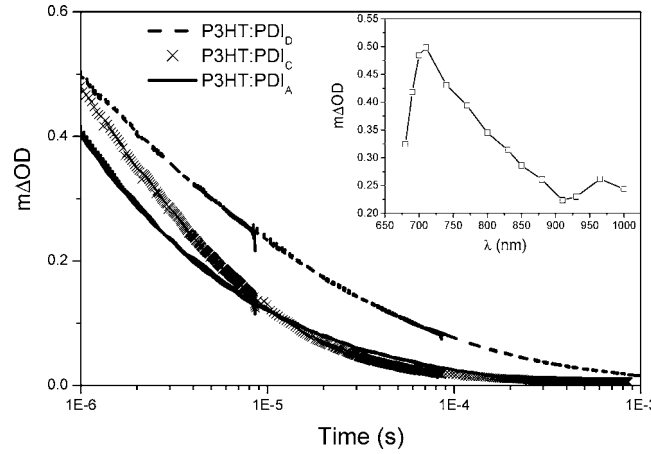

Figure 4. Typical transient absorption data for P3HT:PDI_A, P3HT:PDI_C, and P3HT:PDI_D (1:1) blend films in a N_2 environment, monitored at 700 nm, with $\lambda_{exc} = 520$ nm at 50 μJ cm^{-2}. Inset: spectrum of P3HT:PDI_E at 1 μs under N_2 using $\lambda_{exc} = 520$ nm at 50 μJ cm^{-2}.

absorption features are shown in Figure 4. In all cases, the transients exhibited micro- to millisecond power law ($\Delta OD \alpha t^{-\alpha}$), and oxygen-independent decay dynamics, consistent with their assignment to polaron rather than triplet absorption (further data, including log/log plots confirming the power law nature of these dynamics are shown in the Supporting Information). Control data on pristine P3HT and PDI films gave negligible transient signals on the time scales studied. As we have discussed extensively previously, and confirmed by numerical modeling,[21,22,32] such power law kinetics on the micro- to millisecond time scales are characteristic of bimolecular recombination of dissociated charge carriers. Such bimolecular recombination kinetics can be readily distinguished from the geminate recombination in such blend films, which exhibit exponential decay dynamics characteristic of such monomolecular processes on the nanosecond (and faster) time scales, as we and others have shown previously.[48] We therefore assign these absorption transients to the bimolecular recombination of dissociated polarons.

Power law ($\Delta OD \alpha t^{-\alpha}$) absorption transients (with $0.38 < \alpha < 0.50$), similar to those shown in Figure 4, were observed for all P3HT:PDI_X films. While similar dynamics were observed for all films, the amplitude of these absorption transients varied significantly. For convenience, we quantify these different signal intensities by the magnitude of the PDI anion absorption at 700 nm at a time delay of 1 μs (corresponding to the time delay used in our previous studies of polymer: PCBM blend films[22] and approximating to the typical time scale for charge collection in such donor/acceptor blend devices). The amplitudes of observed decay transients were observed to vary approximately linearly with excitation density (see the Supporting Information), indicating that neither saturation effects nor bimolecular losses prior 1 μs significantly distorted this comparison. These ΔOD

(39) Mizuguchi, J. *J. Appl. Phys.* **1998**, *84*, 8.
(40) Foster, S.; Finlayson, C. E.; Keivanidis, P. E.; Huang, Y. S.; Hwang, I.; Friend, R. H.; Otten, M. B. J.; Lu, L. P.; Schwartz, E.; Nolte, R. J. M.; Rowan, A. E. *Macromolecules* **2009**, *42*, 2023.
(41) Howard, I. L., F.; Keivanidis, P.; Friend, R.; Greenham, N. *J. Phys. Chem. C* **2009**, *113*, 21225.
(42) Giaimo, J. M.; Gusev, A. V.; Wasielewski, M. R. *J. Am. Chem. Soc.* **2002**, *124*, 8530.
(43) van der Boom, T.; Hayes, R. T.; Zhao, Y.; Bushard, P. J.; Weiss, E. A.; Wasielewski, M. R. *J. Am. Chem. Soc.* **2002**, *124*, 9582.
(44) Korovyanko, O. J.; Österbacka, R.; Jiang, X. M.; Vardeny, Z. V.; Janssen, R. A. J. *Phys. Rev. B* **2001**, *64*, 235122.
(45) Österbacka, R.; An, C. P.; Jiang, X. M.; Vardeny, Z. V. *Science* **2000**, *287*, 839.
(46) Riedel, I.; von Hauff, E.; Parisi, J.; Martín, N.; Giacalone, F.; Dyakonov, V. *Adv. Func. Mater.* **2005**, *15*, 1979.
(47) Westerling, M.; Österbacka, R.; Stubb, H. *Phys. Rev. B* **2002**, *66*, 165220.
(48) Shoaee, S.; Eng, M. P.; Espildora, E.; Delgado, J. L.; Campo, B.; Martin, N.; Vanderzande, D.; Durrant, J. R. *Energy Environ. Sci.* , *3*, 971.

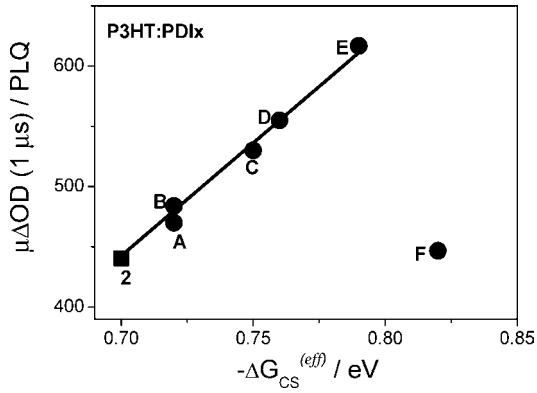

Figure 5. Transient absorbance signal measured at 1 μs of various P3HT:PDI_X (1:1) blend films with P3HT plotted against $-\Delta G_{CS}^{eff}$, estimated as $E_S - (IP_D - EA_A)$. The transient signal has been corrected for variation in the optical absorbance at the excitation wavelength (500 nm) and the PL quenching. $\lambda_{prb} = 700$ nm at 50 μJ cm^{-2}.

signal intensities are summarized in Table 1, normalized for variations (<±35%) in the density of absorbed photons due to variations in film optical density at the excitation wavelength). It is apparent that these changes in ΔOD signal intensities, and therefore yield of dissociated polarons, do not correlate with the variation in PL quenching observed between the blend films. As such, these variations in polaron yields cannot be assigned primarily to changes in the efficiency of exciton dissociation $\eta_{DISS(EXC)}$. Rather, as we have concluded previously for other materials systems,[22,23,25,26] the observation variation in polaron yield is more reasonably assigned primarily to variations in geminate recombination losses on the pico to nanosecond time scales and thus to the variations in the efficiency of dissociation of interfacial CT states into free charges, $\eta_{DISS(CT)}$.

We turn now to consideration of the extent to which the observed variation in polaron yield can be correlated with variations in interfacial energetics. In this regard, we normalized the ΔOD data to take account of the (small) variations in PL quenching, and thus $\eta_{DISS(EXC)}$, observed between the blend films, as detailed as in Table 1 as ΔOD/PLQ. As such, ΔOD/PLQ should be a direct indicator of the efficiency of dissociation of initially generated interfacial polarons into dissociated charges, $\eta_{DISS(CT)}$. Figure 5 shows a plot of the correlation between this assay of charge-transfer state dissociation and the energetic driving force for charge separation $\Delta G_{CS}^{eff} = E_S - (IP_D - EA_A)$. Estimates were performed using either the P3HT or PDI_X singlet energies for E_S. Employing the PDI_X singlet energies, no correlation was observed between ΔG_{CS}^{eff} and the ΔOD/PLQ signal magnitude, suggesting that the charge separation does not proceed from PDI singlet excitons, consistent with our discussion above of absorption and PL emission spectra. However, employing the P3HT S_1 singlet exciton energy for E_S, a remarkably good correlation is observed between ΔG_{CS}^{eff} and ΔOD/PLQ. With the exception of PDI_F (discussed below), the polaron yield, and thus $\eta_{DISS(CT)}$, is observed to show a linear dependence upon ΔG_{CS}^{eff}, increasing by ∼40% for a 0.1 eV increase in driving force. The variation in ΔG_{CS}^{eff} between the different blend films results solely from variations in the PDI electron affinities, as both E_S and IP_D correspond to the P3HT, which is invariant for this film series. We thus conclude that for this materials series there is generally an excellent correlation between the LUMO energy level of the acceptor and the yield of dissociated polarons.

It is striking that, compared to our previous studies of the correlation between polaron yield and ΔG_{CS}^{eff} as a function of donor polymer, the correlation observed in Figure 5 shows remarkably little deviation from a direct linear dependence. The lack of "noise" in this correlation can be primarily attributed to the use of the well-defined, and relatively invariant, PDI anion absorption band (in contrast to our previous studies based upon polymer polaron absorption) and to our correction for small variations in PL quenching (and $\eta_{DISS(EXC)}$) between blend films studied. In this regard, we extended our previous study of polythiophene/PDI_2 blend films[21] to polythiophene/PDI_D blend films, monitoring the ΔOD signal at the PDI anion absorption maximum, and normalizing for variations in PL quenching as above, as shown in the Supporting Information (Table S1) and Figure 7 below. Again a correlation between ΔG_{CS}^{eff} and ΔOD/PLQ is observed, although in this case, the correlation is less well-defined than that observed in Figure 5, presumably due to other factors varying between the polymers to influence charge dissociation in addition to ΔG_{CS}^{eff}.

It is apparent from Figure 5 that the P3HT:PDI_F blend film shows an anomalously low polaron yield considering its relatively large value for ΔG_{CS}^{eff}. In this regard, we note that other 1,7-dibromo PDIs have been found to be severely distorted from planarity by the interaction of the two bulky bromine substituents in the 1 and 7 positions with the hydrogen atoms in the 2 and 6 positions. In particular an analogous dibromo PDI has been found to exhibit poorly stacked solid-state structures and an anomalously low electron mobility relative to the other PDIs with less bulky 1,7-substituents.[49] Furthermore, the disruption of π stacking seen in other dibromo PDIs might lead to a different relation between solution reduction potential and EA vs the other PDIs. We have previously proposed that the relatively high polaron yields observed for polythiophene: PDI_2 blend films relative to polythiophene: PCBM blend films could result from the higher electron mobility of PDI_2 relative to PCBM.[21] As such, the lower polaron yield observed for PDI_F provides further support for this proposition, with its lower charge dissociation efficiency being consistent with the lower electron mobility found for analogous 1,7-dibromo PDI.

Discussion

The results presented herein builds upon our previous studies which have indicated that a key parameter determining the efficiency of charge photogeneration in polymer/small molecule blend films is the energetic driving force for charge separation ΔG_{CS}^{eff}. In particular, we have extended our previous studies as a function of donor polymer ionization potential and singlet exciton energy[22] to a study as a function of acceptor electron affinity. For the PDI acceptor series studied herein, a remarkably good correlation is observed between the efficiency of charge photogeneration, as determined by a transient absorption assay of the dissociated polarons, and ΔG_{CS}^{eff}. We discuss first of all the charge-separation model that we have proposed to explain such energetic correlations, and then go on to make a quantitative comparison of the correlation we observe herein with those we have reported previously for polymer:PCBM blend films.

Figure 6 summarizes a kinetic model for charge photogeneration in donor/acceptor systems, proceeding via the formation of an interfacial bound polaron pair or 'charge-transfer' state,

(49) Jones, B. A.; Facchetti, A.; Wasielewski, M. R.; Marks, T. J. *J. Am. Chem. Soc.* **2007**, *129*, 15259.

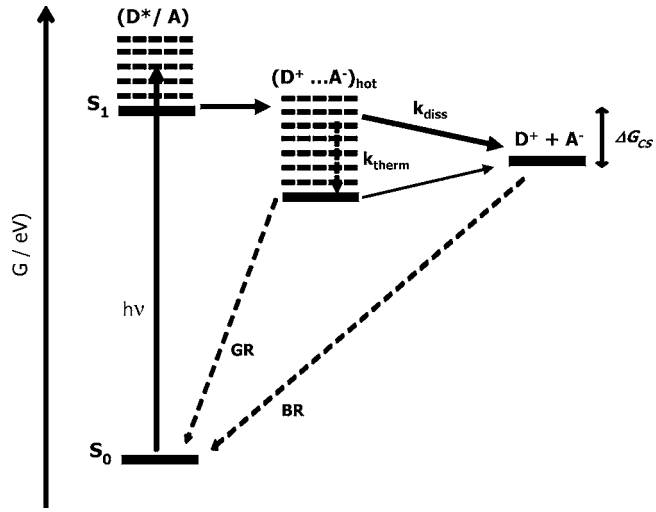

Figure 6. Energy diagram for charge formation in a donor/acceptor (D/A) system via a bound ($D^+\cdots A^-$) CT state. The initially formed bound CT state ($D^+\cdots A^-)_{hot}$ can either undergo thermalisation (k_{therm}) or dissociation (k_{diss}) into the free charge carriers $D^+ + A^-$, which can then contribute to the device current. Charges can recombine either by geminate (GR) or bimolecular (BR) recombination. We note that bimolecular recombination is likely to proceed via reformation of interfacial CT states.

as we and others have proposed previously.[22,23,50,57] We note that a similar model has previously been proposed to describe magnetic field and other effects on charge photogeneration in neat conjugated polymers.[51,52] The model shown in Figure 6 is based upon our experimental observation that while polymer excitons are usually efficiently quenched at the donor/acceptor interfaces for all the blend films considered herein, the final yield of dissociated charges is dependent upon the exciton energy E_S relative to the energy of the dissociated polaron pairs (as defined by $IP_D - EA_A$). Following this model, the initial charge separation of the exciton results in the formation of a vibrationally excited ("hot") CT state, analogous to the "crossing point" in Marcus electron-transfer theory. The Coulombic attraction of these CT states results in a significant potential energy barrier to their dissociation, as we discuss in detail elsewhere in terms of a charge-transfer state binding energy.[53] The model is based upon the concept that the excess thermal energy of the initially formed hot CT state can enable the dissociation of the CT state into free charges.[54] As such, the magnitude of the excess vibrational energy (which can be expected to be proportional to ΔG_{CS}^{eff}) can be expected to correlate with the efficiency of CT state dissociation $\eta_{DISS(CT)}$, consistent with the correlation we observe experimentally in Figure 5. Within this model, the key kinetic competition in the photogeneration process is between vibrational relaxation (k_{therm}) of the initially generated hot CT state and dissociation (k_{diss}) of this species. CT states which thermally relax prior charge dissociation are likely to undergo geminate recombination, with this monomolecular process thus being the primary charge carrier loss pathway. We note that it may also be possible for relaxed CT states to dissociate into free charges, although the importance of this pathway in the overall process of charge photogeneration is currently unclear.

The model detailed in Figure 6 is analogous to Onsager's theory of charge photogeneration applied to a donor/acceptor interface. Onsager theory was originally developed to describe the probability that a photogenerated electron−hole pair in a weak electrolyte would escape its Coulomb attraction and dissociate into free charges.[55] Specifically, the theory proposed that photon absorption generates a localized hole and a hot electron; the latter, due to its excess thermal energy then undergoes rapid motion until it thermalizs at distance a (the thermalisation length) from the localized hole. The resultant electron−hole pair is analogous to the interfacial CT states referred to herein. The competition between dissociation of this electron/hole pair and its geminate recombination back to the ground state depends upon the magnitude of the Coulombic interaction felt by this species. Onsager proposed a definition for a coulomb capture radius (also called the Onsager radius), r_c: the distance at which the Coulomb attraction energy equals the thermal energy k_BT. If the thermalisation length a is greater than the coulomb capture radius, then the charge carriers can dissociate efficiently. If, however, the thermalisation length is smaller than r_c, then the dissociation of the CT state into free charges occurs with an escape probability of $P(E)$ while geminate recombination to regenerate the ground state occurs with a probability of $1 - P(E)$.

Onsager theory can be translated directly to charge photogeneration at the donor/acceptor interfaces studied herein. In general, the exciton will undergo vibrational relaxation prior to charge separation at the donor/acceptor interface (except for direct photoexcitation at the interface). However, due to the offset of donor and acceptor LUMO levels, the electron injected in the acceptor will initially be thermally hot. It is therefore plausible that the same consideration of the electron's thermalisation length versus coulomb capture radius r_c can be applied to determine the yield of charge photogeneration at donor/acceptor interfaces. We note that in this context, calculation of r_c should take account of the polaronic nature of the charge carriers, and the energetic disorder present in such materials. As such, a reasonable estimate for r_c is likely to be of the order of 5 nm, as we discuss in detail elsewhere.[53]

In this context, the correlation between ΔG_{CS}^{eff} and polaron photogeneration efficiency, and thus $\eta_{DISS(CT)}$, that we observe herein can be understood in terms of the influence of ΔG_{CS}^{eff} upon the excess thermal energy of the injected electron and, thus, upon the electron thermalisation length a. This concept of the energy-level offset at the interface influencing the thermalisation length has been proposed previously. In particular, Peumans and Forrest[31] used Monte Carlo calculations based upon Onsager theory to simulate the dissociation of charges at a donor/acceptor interface. Their model assumed that the electron was injected with an excess thermal energy corresponding to the LUMO level offset (approximating to ΔG_{CS}^{eff}). These calculations were consistent with photocurrent generation efficiencies in small molecule bilayer organic solar cells. Furthermore, recent ultrafast transient vibrational spectroscopic data reported by Pensack and Asbury[56] on a polymer/PCBM blend system indicate barrierless free charge carrier formation, suggesting that it is the excess

(50) Westenhoff, S.; Howard, I. A.; Hodgkiss, J. M.; Kirov, K. R.; Bronstein, H. A.; Williams, C. K.; Greenham, N. C.; Friend, R. H. *J. Am. Chem. Soc.* **2008**, *130*, 13653.
(51) Frankevich, E. L.; Lymarev, A. A.; Sokolik, I.; Kaasz, F. E.; Blumstengel, S.; Baughman, R. H.; Horhold, H. H. *Phys. Rev. B* **1992**, *46*, 9320.
(52) Rothberg, L. J.; Yan, M.; Papadimitrakopoulos, F.; Galvin, M. E.; Kwock, E. W.; Miller, T. M. *Synth. Met.* **1996**, *80*, 41.
(53) Clarke, T.; Durrant, J. *Chem. Rev.* **2010**, in press.
(54) Zhu, X. Y.; Yang, Q.; Muntwiler, M. *Acc. Chem. Res.* **2009**, *42*, 1779.
(55) Onsager, L. *Phys. Rev.* **1938**, *54*, 554.
(56) Pensack, R. D.; Asbury, J. B. *J. Am. Chem. Soc.* **2009**, *131*, 15986.

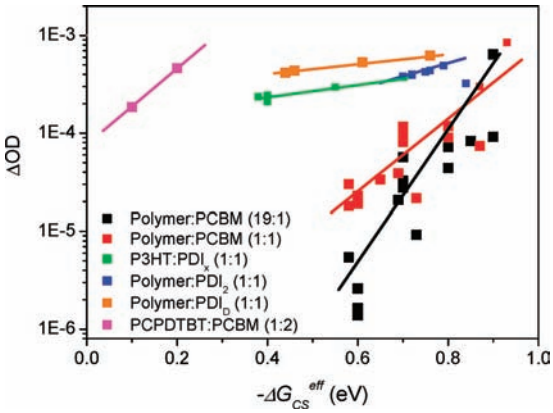

Figure 7. Plot showing the correlation between our transient absorbance assay of the yield of dissociated charges and the energy difference driving charge photogeneration for six different donor/acceptor materials series evaluated from the amplitude of the transient absorbance power law decay at 100 ns (data determined at 1 μs and 100 ns give essentially indistinguishable plots). ΔOD signal amplitude has been normalized to account for differences in film absorption at the excitation wavelength, excitation energy density (with all points being collected at excitation densities low enough to avoid saturation effects). Data for the P3HT:PDI$_X$, polymer:PDI$_D$ and polymer:PDI$_2$ series are reported herein, and include correction for PL quenching efficiency, as detailed above. These two data series employed a 700 nm probe wavelength to monitor the PDI anion absorption; all other data series probed the NIR polymer polaron absorption maximum, typically at 980 nm. The data employing 700 nm probe have been normalized to account for the relative high PDI anion extinction coefficient relative to typical polymer polarons. Data for the polymer:PDI$_2$ are taken from ref,[29] with the additional correction for PL quenching efficiency. Data for the three PCBM based series have been reported previously.[22,25,26,28] The electron affinities of the PDIs have been normalized against that of PCBM, assuming its electron affinity to be 3.7 eV.

vibrational energy in the CT that enables it to overcome its Coulombic interaction.[54,57] This is consistent with the energetic model proposed in Figure 6.[53,58]

We turn now to a comparison of the results we report herein for the P3HT:PDI$_X$ series against those we have observed previously for polymer:PCBM blend films. Figure 7 presents an overview of these data, plotting the charge-generation yield, as measured by transient absorption spectroscopy, versus ΔG_{CS}^{eff} for all the materials series we have studied to date. These include not only studies of the 1:1 polythiophene: PDI films as detailed herein,[21] but also studies of 19:1[22] and 1:1[23] polythiophene: PCBM blend films and PCPDTBT: PC$_{70}$BM blend films with and without added 1,8-octanedithiol.[25] As detailed above, the series employing PDI acceptors have been corrected for differences in PL quenching; this correction was not necessary for the PCBM data series due to the consistently higher PL quenching observed for these series. The data in this figure have also been normalized to account for the higher PDI anion extinction coefficient compared to that of the polymer polaron absorption monitored in our previous studies. Two points are most obviously apparent from this figure. First of all, it is apparent for all the materials series studied; there are clear correlations between ΔG_{CS}^{eff} and ΔOD. Second it is apparent that quantitative strength of these correlations and the absolute magnitudes of ΔOD for a given ΔG_{CS}^{eff} vary substantially between materials series. The first observation, of the correlation between ΔG_{CS}^{eff} and ΔOD within each data series, supports the generality of the hot CT state model we propose above, as summarized in Figure 5. The second observation, of the differences between materials series, requires further discussion.

In general, the Onsager-based charge separation model detailed in Figure 6 suggests that charge photogeneration should be dependent upon a range of parameters. The electron thermalisation length a can be expected to depend not only or the amount of excess thermal energy (and therefore ΔG_{CS}^{eff}) but also the electron mobility and thermalisation time scale.[58] The coulomb capture radius can be expected to depend upon the local dielectric constant. Furthermore, the dissociation yield is likely to be dependent upon the molecular structure of the interface, and in particular the spatial separation of the initially generated CT state, the physical size of the donor and acceptor domains (particular if these are less than r_c), the potential presence of macroscopic electric fields and the rate constant for geminate recombination. In this context, it is remarkable that it is possible to observe such clear correlations between polaron yield and ΔG_{CS}^{eff} within each materials series shown in Figure 7. This observation implies that within each such materials series, the key parameter changing within the series is ΔG_{CS}^{eff} and that all the other parameters likely to influence $\eta_{DISS(CT)}$ are relatively invariant within the data spread ("noise") apparent within each series. In this regard it is interesting to note that we have shown that variations in charge photogeneration following annealing of P3HT:PCBM blend films and the use of a dithiol cosolvent in PCPDTBT:PC$_{70}$BM blend films both correlate with changes in ΔG_{CS}^{eff}. In both cases, the increase in charge photogeneration (and current) was assigned to a reduction in IP resulting from increased polymer crystallization. We note that recent studies have also reported reductions in P3HT IP upon thermal annealing,[23] consistent with these observations. As such it appears clear that ΔG_{CS}^{eff} is a key parameter determining charge photogeneration yield in such blend films.

Turning now to consideration of the differences between materials series plotted in Figure 7, these can be assigned to the other factors influencing $\eta_{DISS(CT)}$ in addition to ΔG_{CS}^{eff}. We have previously proposed that the significant increase in the yield of dissociated charges in polymer/PDI blend films relative to polymer: PCBM blends with equivalent ΔG_{CS}^{eff} may result from the higher electron mobility of the PDI's employed,[21] which can be expected to increase the electron thermalisation length.[59] This highlights the potential importance of the charge-carrier mobility not only in transport but also to facilitate charge photogeneration. Interestingly, we have previously noted that the charge photogeneration yield did not show a significant correlation with polymer hole mobility.[22] This distinction most probably derives from charge separation in these blends primarily involving LUMO to LUMO electron transfer, with acceptor electron mobility thus being the critical parameter. Turning to comparisons of the other materials series, the high charge photogeneration yields for the donor−acceptor polymer PCPDTBT is indicative of the charge transfer character of this polymer faciliting dissociation of the CT state, either by the effective introduction of a redox cascade at the donor/acceptor interface or modulation of the local dielectric constant.[25] The higher charge photogeneration yields observed for 1:1 compared to 19:1 polythiophene:PCBM blends is consistent with the larger PCBM domains in the 1:1 blends facilitating charge dissociation.[23] Clearly these comparisons are limited in their scope, and

(57) Brédas, J.-L.; Norton, J. E.; Cornil, J.; Coropceanu, V. *Acc. Chem. Res.* **2009**, *42*, 1691.
(58) Morteani, A. C.; Sreearunothai, P.; Herz, L. M.; Friend, R. H.; Silva, C. *Phys. Rev. Lett.* **2004**, *92*, 247402.
(59) Peng, Y.-Q.; Lu, F.-P. *Appl. Surf. Sci.* **2006**, *252*, 6275.

provide only partial insights into the range of parameters which influence charge photogeneration in polymer: small molecule blend films. Nevertheless they do provide some insights into the key materials properties influencing charge photogeneration in such blend films.

These results demonstrate that in comparisons of charge (or photocurrent) photogeneration between materials, several factors may potentially influence charge photogeneration in addition to ΔG_{CS}^{eff}. In this regard, it is interesting to note that efficient photocurrent generation, and higher devices voltages, have been reported for polymer/fullerene blend solar cells employing fullerenes with lower electron affinities than PCBM. The lower electron affinities result in a lower ΔG_{CS}^{eff} and thus might be expected to result in lower photocurrent generation. The observation of efficient photocurrent generation suggests that additional factors are enhancing photocurrent generation in this case, such as, for example, the interface molecular structure, although at present it is unclear what these factors are.

The study herein has focused upon the charge photogeneration process in blend films, rather than the overall process of photocurrent generation. In particular, it does not include consideration of the charge collection efficiency η_{COLL}. We have previously shown for both P3HT:PCBM and PCPDTBT:$PC_{70}BM$ blend films that there is a correlation between our transient absorption assay of charge photogeneration and photocurrent density, suggesting that charge photogeneration rather than collection is the key determinant of photocurrent density in these devices.[23,26] However, for polymer/PDI based devices, it has previously been reported that charge collection is the dominant factor limiting device performance; low currents have been attributed to unfavorable blend nanomorphologies preventing efficient polaron collection at the device electrodes.[60−64] In this regard, it is interesting to note that P3HT:PDI_D based devices exhibited substantially higher photocurrent densities than P3HT:PDI2 based devices (see the Supporting Information), consistent with the differences in film nanomorphologies shown in Figure 3. Nevertheless, the photovoltaic device performance for devices based upon P3HT:PDI_X blends films exhibited only modest device performance, consistent with previous studies of polymer/PDI based devices. In this regard, we note that the high charge photogeneration efficiencies we observe for polymer/PDI blend films, coupled with the strong light absorption and excellent stability of PDIs, suggest that if the collection limitations imposed by unfavorable nanomorphology can be addressed then PDIs may indeed be attractive alternatives to PCBM in organic bulk heterojunction solar cells.

Concluding Remarks

The results reported in this paper provide further evidence that a key factor determining the efficiency of charge photogeneration at in organic donor/acceptor blend films is the free energy difference driving charge separation, referred to herein as ΔG_{CS}^{eff}. In particular we demonstrate that for a series of electron acceptors with differing electron affinities, there is a direct correlation between the acceptor LUMO level and the efficiency of charge dissociation. This dependence is not correlated with the efficiency of exciton quenching at this interface (as measured by polymer exciton photoluminescence quenching) but rather assigned to the dissociation of interfacial charge transfer states being dependent upon the excess thermal energy of the initially generated CT state.

More generally, we have now observed clear correlations between charge photogeneration yield and ΔG_{CS}^{eff} for 6 different donor:acceptor materials series, as shown in Figure 7, providing clear evidence that this energetic dependence is a key factor determining charge photogeneration efficiency for many organic blend films. Moreover, we further find that differences in charge photogeneration between materials series can not attributed to this energetic dependence. Rather such differences between materials series are indicators of some of the other factors also influencing charge photogeneration in such blend films, including film nanomorphology, the charge transfer character of the donor polymer and the electron mobility of the acceptor. As such, we are starting to develop a series of materials design rules for charge photogeneration at organic donor/acceptor interfaces which can be employed to aid materials and blend nanomorphology design for increasing the performance of organic solar cells.

Acknowledgment. The authors are grateful to Solvay S.A., the UK's EPSRC and OST for financial support. Work was also supported by STC Program of the NSF (DMR-0120967) and by the ONR (N00014-04-1-0120). We also thank Dr Keivanidis and Professor Nelson for helpful discussions.

Supporting Information Available: Experimental details, electrochemical data, nanomorphology, some photophysical and properties of polymer:PDI_X, and device data. This material is available free of charge via the Internet at http://pubs.acs.org.

JA1042726

(60) Conboy, J. C.; Olson, E. J. C.; Adams, D. M.; Kerimo, J.; Zaban, A.; Gregg, B. A.; Barbara, P. F. *J. Phys. Chem. B* **1998**, *102*, 4516.
(61) Adams, D. M.; Kerimo, J.; Olson, E. J. C.; Zaban, A.; Gregg, B. A.; Barbara, P. F. *J. Am. Chem. Soc.* **1997**, *119*, 10608.
(62) Dittmer, J. J.; Marseglia, E. A.; Friend, R. H. *Adv. Mater.* **2000**, *12*, 1270.
(63) Rajaram, S.; Armstrong, P. B.; Kim, B. J.; Fréchet, J. M. *J. Chem. Mater.* **2009**, *21*, 1775.
(64) Keivanidis, P.; Howard, I.; Friend, H. R. *Adv. Func. Mater.* **2008**, *18*, 1.